

Research paper

## Semi-solid extrusion 3D-printing of eucalypt extract-loaded polyethylene oxide gels intended for pharmaceutical applications

Oleh Koshovyi<sup>a,b,\*</sup>, Jyrki Heinämäki<sup>a</sup>, Ivo Laidmäe<sup>a</sup>, Niklas Sandler Topelius<sup>c</sup>,  
Andriy Grytsyk<sup>d</sup>, Ain Raal<sup>a</sup>

<sup>a</sup> Institute of Pharmacy, Faculty of Medicine, University of Tartu, Nooruse 1, 50411 Tartu, Estonia

<sup>b</sup> The National University of Pharmacy, 53 Pushkinska st, 61002 Kharkiv, Ukraine

<sup>c</sup> CurifyLabs Oy, Salmisaarenaukio 1, 00180 Helsinki, Finland

<sup>d</sup> Ivano-Frankivsk National Medical University, 2 Galytska Str., 76018, Ivano-Frankivsk, Ukraine



## ARTICLE INFO

## Keywords:

Eucalypt leaves extract (EE)  
Polyethylene oxide (PEO)  
Aqueous gel  
Semi-solid extrusion (SSE) 3D printing  
Pharmaceutical delivery system

## ABSTRACT

In pharmaceuticals, 3D printing is considered as a promising future technology for fabricating more complex patient-specific drug delivery systems (DDSs). An anti-staphylococcal herbal preparation, “Chlorophyllipt”, is produced mainly in a liquid form by the pharmaceutical industry in Ukraine, and it is composed of an ethanolic eucalypt extract (EE). Since staphylococcal infections have become a true challenge for the health care in all over the world, it would be relevant and justified to develop the aqueous gels of the present EE applicable for the 3D printing of the corresponding solid DDSs. The aim of the present study was to develop a novel polyethylene oxide (PEO) gel loaded with EE for a semi-solid extrusion (SSE) 3D printing and to print the corresponding oral solid DDSs with different sizes and shapes. For SSE 3D printing, we prepared and tested total ten (10) different aqueous PEO gel formulations loaded with EE. Prior to 3D printing, the physical appearance, homogeneity, injection force and viscosity of the gels were investigated. The EE-PEO gels were printed to lattice- and round-shaped solid DDSs with the head speed of 0.5 mm/s, and the weight (mass uniformity) and effective surface area of the printed systems were determined. The most feasible EE-PEO gel for SSE 3D printing comprised of 10 mg/ml of EE, 30 mg/ml of eumulgin and 20 mg/ml of ascorbic acid in a 20-% aqueous PEO gel. The key process parameters of the SSE 3D printing were identified and verified. The printing quality of EE-PEO DDSs were very good, thus showing compatibility of a plant extract and carrier polymer. Such 3D-printed antimicrobial DDSs can be used for example in the treatment of skin wounds and infections of the oral cavity.

### 1. Introduction

The “one size fits all” conception is still common in medicine, but within the recent years, the new paradigm of a personalised medicine is becoming more and more popular. It is an approach to enhance the prevention, diagnosis and treatment of diseases to benefit a specific group of patients, such as children and elderly people, who need pharmaceutical dosage forms different from the average ones. One important “pharmaceutical tool” for fostering the implementation of personalized medicine in medicine is 3D printing. In pharmaceutical 3D printing, by using different carrier polymers and excipients, it is possible to formulate novel tailor-made drug delivery systems (DDSs) and to modify the drug release behaviour. Therefore, 3D printing as a versatile additive manufacturing technique holds great promises in pharmaceuticals for

designing and fabricating advanced patient-specific DDSs [1–5].

In the past recent years, 3D printing is increasingly used in various medical disciplines. One specific field in medicine, where 3D printing has found wide uses and advances is surgery [6]. Modern 3D printing principles were also used before implementing 3D printing in the successful manual recreation of urinary bladder [7]. Printing technologies have found also promising applications in the other medical specialties, such as cardiology [8,9], dentistry [10], urology [11,12] and plastic surgery [13].

In pharmaceuticals, 3D printing has been used to produce polypills containing five or even more active pharmaceutical ingredients (APIs) in the same drug preparation [14,15]. Pharmaceutical 3D printing was also successfully applied for modifying and tailoring the drug release patterns of APIs in such oral solid DDS [14,15]. In 2015, US Food and Drug

\* Corresponding author at: 53 Pushkinska str., 61002 Kharkiv, Ukraine.

E-mail address: [oleh.koshovyi@ut.ee](mailto:oleh.koshovyi@ut.ee) (O. Koshovyi).

<https://doi.org/10.1016/j.stlm.2023.100123>

Received 12 April 2023; Received in revised form 23 June 2023; Accepted 9 August 2023

Available online 12 August 2023

2666-9641/© 2023 The Author(s). Published by Elsevier Masson SAS. This is an open access article under the CC BY-NC-ND license (<http://creativecommons.org/licenses/by-nc-nd/4.0/>).

Administration (FDA) approved the marketing authorisation application of the first 3D-printed drug product, Spritam® (levetiracetam) oral rapidly disintegrating tablet, intended for the treatment of epilepsy [16]. To date, the APIs formulated into 3D-printed drug products have been mainly purified synthetic substances, and only little is known about the 3D printing of more complex plant-origin materials, such as extracts and herbal mixtures. Such plant-origin materials are often sensitive to higher temperatures and organic solvents and/or water, which causes additional challenges for a 3D printing process. To date, there are only a few studies published on the pharmaceutical 3D printing of plant extracts [17,18,19].

Since many plant-origin materials are known to be sensitive to higher temperatures, a semi-solid extrusion (SSE) 3D-printing method is the method of choice for such printings. A SSE 3D printing, also called as pressure-assisted micro syringe (PAM) or micro-extrusion-based printing, can be performed at a room temperature without any heating [20, 21,22]. A syringe-like printing head containing a printing material is moved around a printing plate at a pre-set speed and trajectory. The material is pushed out of the printing head at a set force level aided by either a screw, piston or pneumatic movement. The selection of a proper driving mechanism is important especially when printing living cell-incorporated materials. The material deposited on a printing plate needs to be dried/solidified before the addition of a subsequent layer [1]. To our best knowledge, a SSE 3D-printing method is also the most feasible selection for formulating novel 3D-printed DDSs containing an antimicrobial eucalypt extract as a plant-origin active material.

Overcoming the health threatening consequences of staphylococcal infections and their negative socio-economic effects, have become a priority in the health care all over the world [23,24]. An anti-staphylococcal herbal preparation, “Chlorophyllipt”, is produced in various dosage forms by the pharmaceutical industry in Ukraine. “Chlorophyllipt” consists an ethanolic eucalypt extract (EE), and it is available e.g., as 1% ethanol solution, 2% oil solution, 0.25% solution for injection, spray and tablets [25]. When using a 1% ethanol solution of “Chlorophyllipt” for rinsing, the solution needs to be diluted with cold or boiled water at a ratio of 1:5 [25]. However, this treatment leads to the final preparation, which is (1) non-standardized, (2) has an additional mineral and microbiological load, (3) is unstable during storage, and (4) contains up to 20% of ethanol. All these drawbacks significantly limit the use of such EE preparations for example in paediatrics.

On the other hand, EE has been used for the treatment of oral cavity infections, throat infections and wound healing for many decades, and the efficacy of such extract in these treatments has proven [25,26]. Therefore, the development of aqueous EE containing gels applicable in SSE 3D printing and the corresponding 3D-printed preparations for oral irrigation uses, would be justified and an urgent task. The antimicrobial activity of Eucalyptus essential oil (the major component of EE) has been proven by several researchers [27]. Eucalyptus essential oils and their major constituents exhibit toxicity against a wide range of microbes, including bacteria, fungi, and soil-borne and post-harvest pathogens. Traditional healers use Eucalyptus to treat many illnesses, such as infections, colds, flu, sore throats, bronchitis, pneumonia, aching, stiffness and neuralgia. The antimicrobial activity of Eucalyptus oil is most likely attributed to the presence of compounds such as 1,8-cineole,  $\alpha$ -pinene,  $\beta$ -pinene and limonene [28]. The recent studies have also shown that Eucalyptus essential oil and its major monoterpenes have a true potential for preventing and treating infectious diseases caused by viruses [29].

The aim of the present study was to develop an aqueous gel formulation for the SSE 3D printing of EE, and to design and prepare novel 3D-printed DDSs for EE with an antimicrobial activity. Polyethylene oxide (PEO) was investigated as a gel former and carrier polymer for 3D printing.

## 2. Materials and methods

### 2.1. Plant extract

For preparing the aqueous PEO gel loaded with EE, 1000 ml “Chlorophyllipt” ethanol solution (10 mg/ml) (series 0054497 PJSC “Halychpharm” of Arterium Corporation, Lviv, Ukraine) was evaporated to obtain a high viscosity (“thick”) extract, which was used for the subsequent stages. The extract was purchased from a community pharmacy, thus it is expected to fully correspond to the requirements of the DMF as it was on sale. In addition, we conducted the following in-house quality tests for the extract: UV-spectrum, assay of chlorophylls and main terpenoids ( $\alpha$ -phellandrene: less than 1.5%, 1,8-cineole: not less than 10%, *trans*-pinocarveol: less than 2%, aromadendrene: less than 30%, globulol at least 10% in the volatile fraction.) by GC/MS [26]. Identification of chlorophylls in the extracts was carried out with a two-dimensional thin-layer chromatography (TLC) using hexane - acetone (8:2) and hexane - acetone (8:4) as solvent systems and the reference standard (RS) samples of chlorophylls *a* and *b*. Chlorophylls are red in colour in UV light. The assay of chlorophylls was carried out by spectrophotometric method [30,31].

### 2.2. Preparation of gels

The aqueous gels of PEO (MW approx. 900,000, Sigma-Aldrich, USA) at the concentrations of 12%, 15% and 20%, were used as a formulation platform for the SSE 3D printing of EEs. For preparing such gels, PEO (1.2 g, 1.5 g or 2.0 g) was dissolved in distilled water (10 ml) approximately for at least 13–15 h at an ambient room temperature to form a viscous gel [1]. For preparing a nanoemulsified aqueous eucalypt extract, Eumulgin SMO 20 (polyethylene glycol 40–hydrogenated castor oil, Polysorbate 80) (LOT S721580003, Cognis, France) were used [26]. The EE (0.05 g, 0.1 g, 0.15 g or 0.2 g), eumulgin as a surface active agent (0.15 g, 0.3 g, 0.45 g or 0.6 g, accordingly), and ascorbic acid (UAB “Armila”, Vilnius, Lithuania) (0.1 g, 0.2 g, 0.3 g or 0.4 g, accordingly), were added into 12%, 15% and 20% PEO gels.

### 2.3. Characterisation of gels

The viscosity of gels was determined with a Physica MCR 101 rheometer (Anton Paar, Austria) using a cone-plate geometry. The measurements were carried out at a room temperature (21–25 °C). The viscosity measurements were performed by using a rotational shear test at the different shear rates.

The injectability of printing gels were determined with a Brookfield CT3 Texture analyser (Middleboro, MA, USA) equipped with a TexturePro CT software (AMETEK Brookfield, Middleboro, MA, USA). In the injectability test, the injection force needed for pushing a printing solution (gel) through a 21 G needle, was measured. The injectability of aqueous PEO gels (12%, 15% and 20%) loaded with EE, was investigated. For performing the test, a 3-ml Luer lock Norm-Ject syringe was filled with a 2 ml of test solution. The syringe was securely placed between the fixtures of a texture analyser, and a continuous speed of 0.5 mm/s was used for material extrusion from the syringe. All measurement were carried out in triplicates at room temperature (22 ± 2 °C).

The gel structure and the degree of homogenization were evaluated by taking light microscopy images at 40, 100 and 400 times of magnification (Magtex-T Dual Illum., Medline Scientific, United Kingdom; Industrial Digital Camera UCMOS09000KPB (9.0 MP 1 / 2.4” APTNA CMOS sensor).

### 2.4. 3D printing of eucalypt extract

The PEO gels loaded with EE were directly printed using a bench-top SSE 3D printing system (System 30 M, Hyrel 3D, USA). The printing head consists of a steel syringe with a plunger connected to a stepper

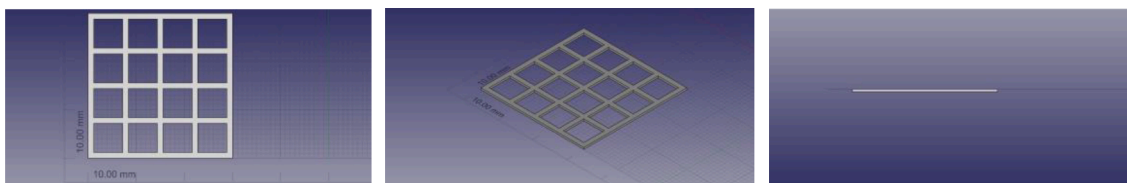


Fig. 1. Computer-aided design (CAD) of lattices.

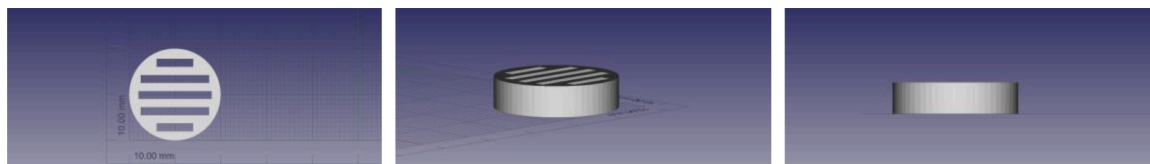


Fig. 2. Computer-aided design (CAD) of rounded shape drug preparations.

motor (the stepper motor moves the plunger up or down and pushes the content in the syringe out). A blunt needle (Gauge, 21 G) connected to syringe serves as a printing nozzle. The printing head (syringe with a nozzle) was not heated. During SSE 3D printing, a printing head moved at a set speed on X-Y axis (= printing speed) and extruded printing material at a specified speed through a nozzle system (= extrusion speed) onto a thermostated printing plate. The printing plate temperature was set at 40 °C. Following every printed layer, a printing plate was lowered by a predefined distance (layer height), thus allowing a printing head to create another layer of material on the top of a printed object. The software of a SSE 3D printer (Repetrel, Rev3.083\_K, Hyrel 3D, USA) controls the temperature of a printing head and plate, the moving speed of a printing head, gel extrusion rate, and other settings. The printing head speeds used were 0.5 mm/s and 1.0 mm/s. Total 8 layers were printed for the model lattices and 5 layers for the round-shaped disc preparations.

For verifying a 3D printing quality, a model 4 × 4 grid lattice (Fig. 1) was designed with an Autodesk 3ds Max Design 2017 software (Autodesk Inc., USA). The dimensions for a square-shaped 3D lattice were 30 × 30 × 0.5 mm. The evaluation of 3D printability was based on the printed lattice weight and area measurements. The theoretical surface area of a square-shaped 3D lattice (324 mm<sup>2</sup>) was compared with the corresponding areas of experimental 3D-printed lattices [1]. A round-shaped disc preparation (20 mm in diameter) (Fig. 2) was

designed by using a FreeCAD software (vers. 0.19 / release date 2021) [32,33].

The 3D-printed PEO lattices and round-shaped disc preparations were weighed with an analytical scale (Scaltec SBC 33, Scaltec, Germany) and photographed. The photographs were analysed with an ImageJ (National Institute of Health, USA) image analysis software (version 1.51k). With the 3D-printed lattices, the experimental value obtained for a surface area was compared with the corresponding theoretical value of a designed lattice. The surface of the 3D-printed round-shaped disc preparations was investigated by means of light microscopy at 40, 100 and 400 times of magnification (Magtex-T Dual Illum., Medline Scientific, United Kingdom; Industrial Digital Camera UCMOS09000KPB (9.0 MP 1 / 2.4" APTNA CMOS sensor).

## 2.5. Statistical analysis

Statistical properties of random variables with n-dimensional normal distribution, are given by their correlation matrices, which can be calculated from the original matrices. Statistical assessment of data is reported as mean ± SEM, and were analysed using MS Excel (Microsoft Excel 2016, version 16.0, Microsoft Corporation, USA). The P values less than 0.05 were considered as statistically significant [34].

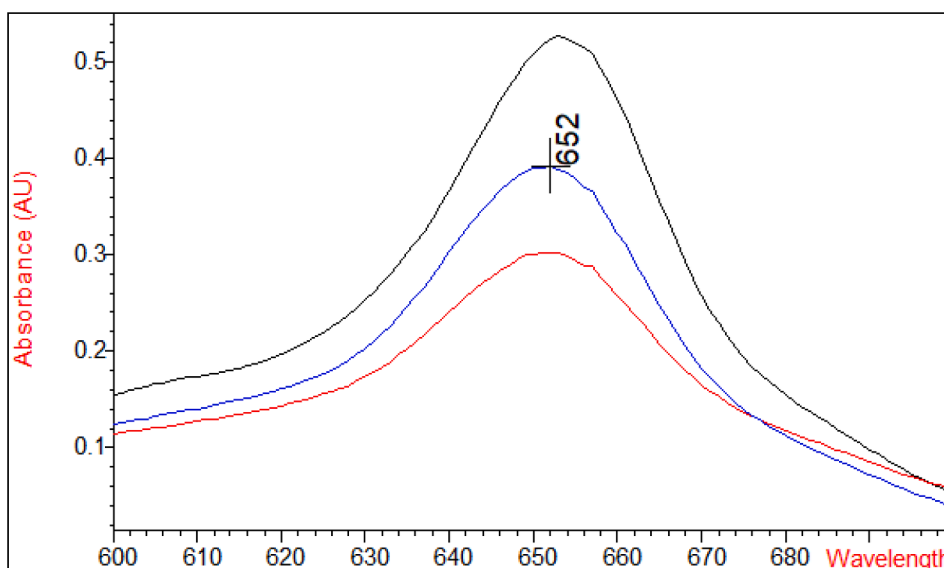


Fig. 3. Ultraviolet (UV) spectrum of eucalypt extract (EE) solution.

**Table 1**

Composition of the aqueous polyethylene oxide (PEO) gels loaded with eucalypt leaves extract (EE). The gels are intended for a semi-solid extrusion (SSE) 3D printing.

Sample	Eucalypt extract, g	Eumulgin, g	Ascorbic acid, g	PEO, g	Water, ml
1	–	–	–	1.21	10.00
2	0.06	0.18	0.14	1.21	10.00
3	0.10	0.29	0.21	1.21	10.00
4	0.15	0.47	0.30	1.21	10.00
5	0.20	0.62	0.41	1.21	10.00
6	0.10	0.29	0.21	1.51	10.00
7	0.05	0.17	0.12	2.00	10.00
8	0.10	0.32	0.22	1.99	10.00
9	0.15	0.44	0.33	1.99	10.00
10	0.20	0.64	0.39	2.01	10.00

**Table 2**

The viscosity and injection force of the aqueous polyethylene oxide (PEO) gels loaded with eucalypt extract (EE).

Sample	Viscosity, cP (Speed 0.3 RPM, Shear rate 0.600 1/s)	The injection force, N
1	623,200±15,795	72.3 ± 5.9
2	229,133±10,701	20.2 ± 0.7
3	234,541±17,281	22.3 ± 1.2
4	274,933±21,293	27.8 ± 0.9
5	270,933±15,263	26.6 ± 3.4
6	459,667±36,757	45.6 ± 2.1
7	578,933±29,582	57.3 ± 9.8
8	617,633±20,420	60.4 ± 1.4
9	632,266±44,297	63.2 ± 2.9
10	568,933±14,858	56.3 ± 1.3

### 3. Results

#### 3.1. Physical appearance and viscosity of aqueous gels

The EE fully corresponded to the requirements of the DMF. Its UV spectrum is presented in Fig. 3 and the maximum of UV spectrum at 652 nm is corresponded to the standard one. The content of chlorophylls was  $2.22 \pm 0.01\%$ , and the main terpenoids were 1,8-cineole 11.1%, globulol 14.7%,  $\alpha$ -phellandrene 1.26%, trans-pinocarveol 1.48%, aromadendrene 26.0% in the volatile fraction.

Since the extract was found to comply with the quality requirements set by the manufacturer and by us (additional quality tests), it was used for the PEO-EE gels intended for SSE 3D printing. Table 1 shows the compositions of the aqueous PEO-EE gels developed for SSE 3D printing. In the gel formulations 3, 6 and 8, the concentration of EE is the same as in the reference commercial pharmaceutical solution, 1% ethanol solution of "Chlorophyllipt"

Physical appearance and homogeneity of aqueous PEO-EE gels were investigated by a visual inspection and light microscopy, respectively. As shown in Fig. 4, the aqueous PEO-EE gels based on 12%, 15% and 20% PEO solution (3, 6, 8, 9, 10) were homogeneous, and also more uniform in structure compared to the other gel formulations studied.

#### 3.2. Viscosity and injection force

The viscosity of aqueous PEO-EE gels were measured, and the results are presented in Table 2. In order to simulate SSE 3D printing, the injection force needed for pushing such PEO-EE gels through a 21 G needle was investigated in a texture analysis system at a room temperature ( $22 \pm 2$  °C), and the results are summarized in Table 2. For example, the changes of viscosity in the PEO gels (# 1, 3, 6, 8) loaded with eucalypt extract in the dose 10 mg/ml are presented in Fig. 5. The injection force changes for the 12% PEO gels during the experiment are shown in Fig. 6.

Based on the results of an injectability test and preliminary SSE 3D printing tests, the printing head speed of choice for the present aqueous PEO-EE gels was found to be 0.5 mm/s.

#### 3.3. SSE 3D printing experiments

The operating parameters for the SSE 3D printing of aqueous PEO gels were recently investigated and optimized by Viidik et al. [1], and we used those results in the development of SSE 3D printing for the gels loaded with EE. We used a blunt needle (Gauge, 21 G). The printing head (syringe with a nozzle) was not heated. The printing plate temperature was set at 40 °C. The printing head speed used was 0.5 mm/s.

The feasibility of the aqueous PEO-EE gels for SSE 3D printing was verified by printing standard size square-shaped 3D lattices with the dimensions of  $30 \times 30 \times 0.5$  mm. Table 3 summarized the weight and surface area of these experimental lattices printed from the aqueous PEO-EE gels (reference is also made to Table 1). The first attempt of SSE

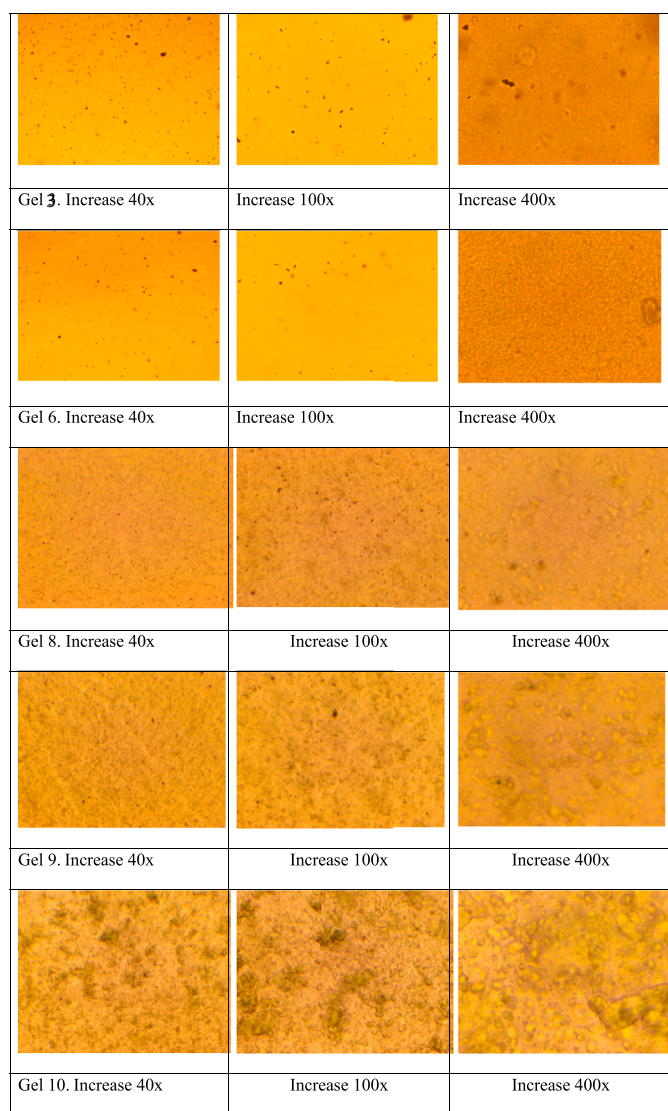


**Fig. 4.** Microscopic analysis of the 12%, 15% and 20% aqueous polyethylene oxide (PEO) gels loaded with eucalypt extract (EE). The magnifications 40 ×, 100 × and 400 ×.



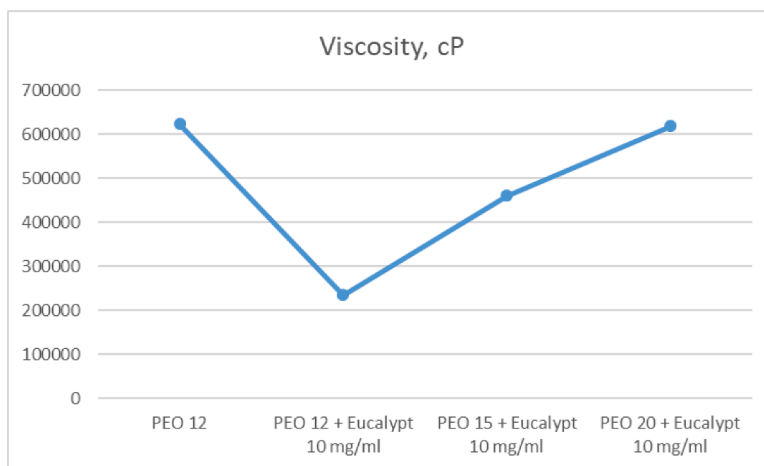


Fig. 5. Changes of viscosity in the PEO gels (12%, 15% and 20%) loaded with the eucalypt extract in the dose of 10 mg/mL.

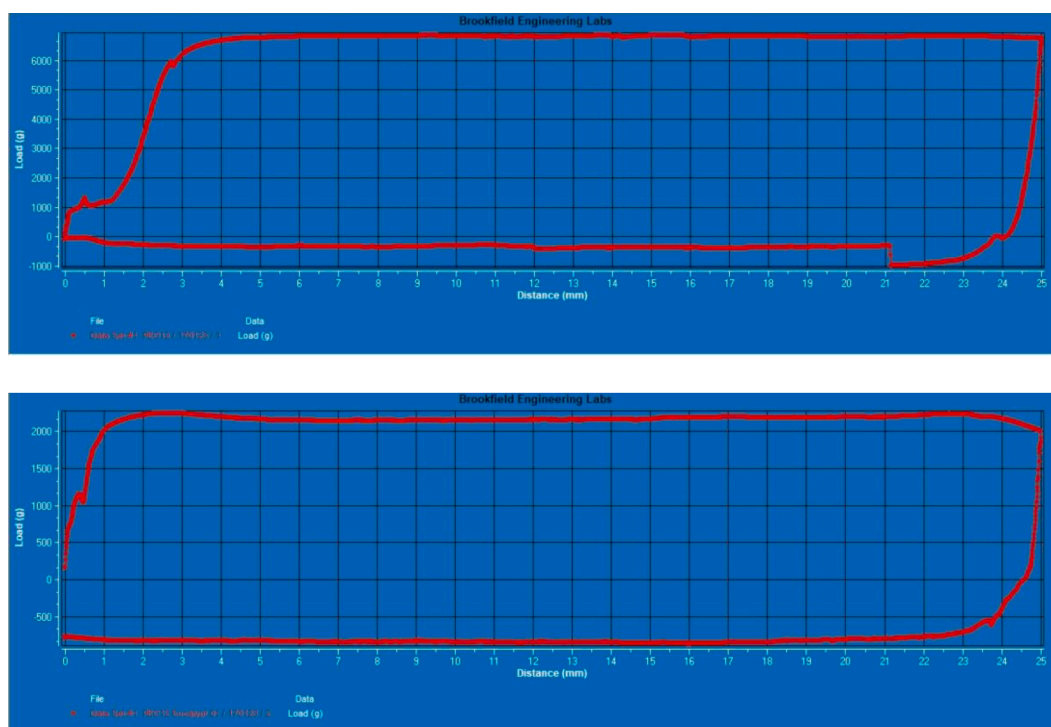


Fig. 6. The injection force changes for the 12% PEO gels (A - 12% PEO gel; B - 12% PEO gel loaded with the eucalypt extract in the dose of 10 mg/mL).

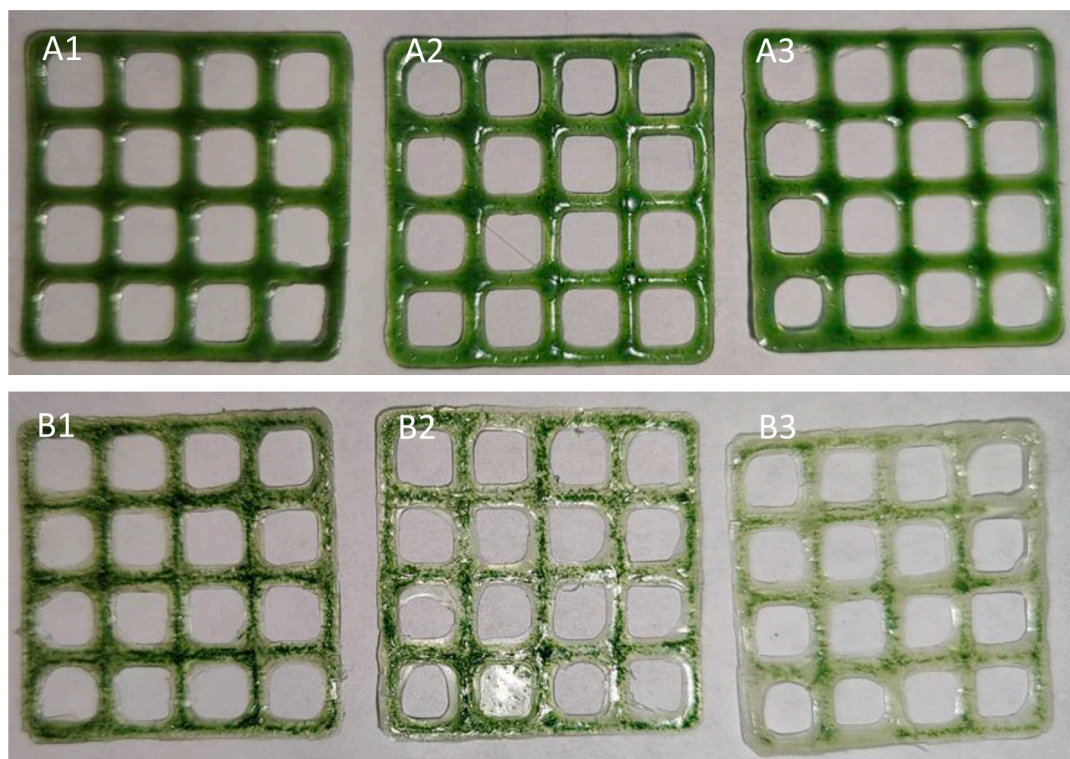
**Table 3**  
Weight and surface area of the semi-solid extrusion (SSE) 3D-printed aqueous PEO lattices loaded with eucalypt extract (EE) (n = 3).

Sample	Weight, g	Area (S), mm <sup>2</sup>	S <sub>practical</sub> / S <sub>theoretical</sub>
1	Reference gel (readily printable) [1]		
2	Failed to print		
3	0.1429±0.0078	573.84±19.23	1.77
4	0.1035±0.0195	595.83±111.00	1.84
5	0.1146±0.0294	607.41±83.25	1.87
6	0.1599±0.0085	515.40±52.12	1.59
7	Failed to print		
8	0.1640±0.0063	404.38±49.71	1.24
9	0.1941±0.028	504.72±66.82	1.56
10	0.2242±0.0025	509.32±28.82	1.57

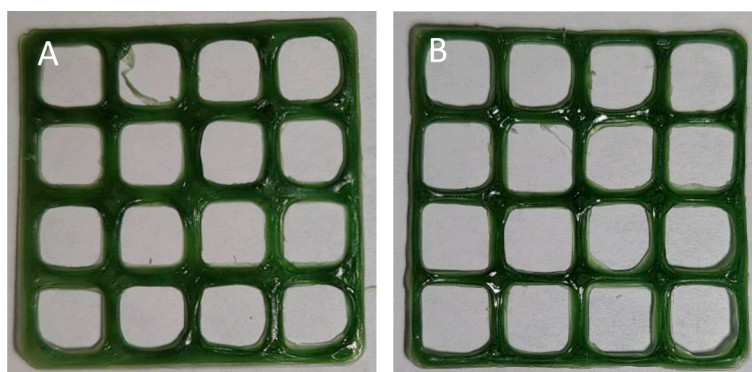
3D printing was carried out with using the gels 2–5 based on the fixed concentration of PEO and with using different concentration of EE. With the gels 4 and 5, a clear layering was observed during a short-term storage, and the viscosity of these gels were low. Moreover, high level of spreading out was noticed with the final 3D-printed lattices (Table 3).

Fig. 7 shows the 3D-printed lattices obtained from the aqueous PEO-EE gels 3 and 5 in three parallel SSE 3D printings. In the 3D printing experiments, the printing head speed was set at 0.5 mm/s, and the total number of layers applied was 8 (Fig. 6). The gel formulation 3 was found to be the most feasible for SSE 3D printing showing very good printing quality and high reproducibility.

Since the 3D printing properties of the 12% aqueous PEO gels with EE were not very good, we attempted to print the gels 6 and 8 (Table 1) with higher concentrations (15% and 20%) of PEO and with 1% of EE, thus simulating the composition of the “Chlorophyllipt” 1% ethanol solution. The 3D printing results of such lattice preparations are presented in Table 3 and Fig. 8.



**Fig. 7.** The semi-solid extrusion (SSE) 3D-printed lattices obtained from the aqueous polyethylene oxide (PEO)-eucalypt extract (EE) gels 3 (A1–3) and 5 (B1–3) in three parallel SSE 3D printings.



**Fig. 8.** The semi-solid extrusion (SSE) 3D-printed lattices obtained from the aqueous polyethylene oxide (PEO)-eucalypt extract (EE) gels 6 (A) and 8 (B) in three parallel SSE 3D printings.

**Fig. 9** shows the 3D-printed lattices obtained from the aqueous PEO-EE gels 9 and 10 in three parallel SSE 3D printings. We found that the 20% aqueous PEO gel loaded with EE presented enhanced SSE 3D printing behaviour over the other gel formulations studied. These findings were also supported by the weight and surface area results of the corresponding 3D lattices summarized in [Table 3](#).

The aqueous PEO (12% and 20%) - EE gels (the compositions shown in [Table 1](#)) were also tested for the SSE 3D printing of round-shaped single-unit disc preparations intended for oral administration ([Table 4](#)). In these preparations, a total number of printed gel layers was five, and the discs were 3D printed with a printing head speed of 0.5 mm/s. [Table 4](#) shows the weight, weight variation and layout (appearance) of the discs. The sample 1 represents the 3D-printed disc preparation (white in colour) generated from the reference aqueous 12% PEO gel without EE ([Table 4](#)).

#### 4. Discussion

The prepared aqueous PEO-EE gels ([Table 1](#)) were all dark green in colour and viscous semisolids with a characteristic smell of 1,8-cineole, which is the main component of eucalypt essential oil. Most of the gels prepared had a fairly homogeneous structure, which was confirmed by the microscopic studies ([Fig. 1](#)). However, in the aqueous PEO-EE gels 4 and 5 ([Table 1](#)), clear signs of stratification and sedimentation were observed even during a short-term storage. Consequently, the 3D printing of these gels was found to be complicated, since a printing head was periodically blocked and the final lattices printed had a non-uniform structure (which was visible even by a naked eye). To solve this printing limitation, it is possible to either increase the viscosity of the gel by adding more PEO, or to increase the amount of surfactant in the gel, but this can lead to a decrease in antibacterial activity.

We found that the addition of eumulgin significantly decreased the viscosity and injection force of the aqueous PEO-EE gels (2–10)

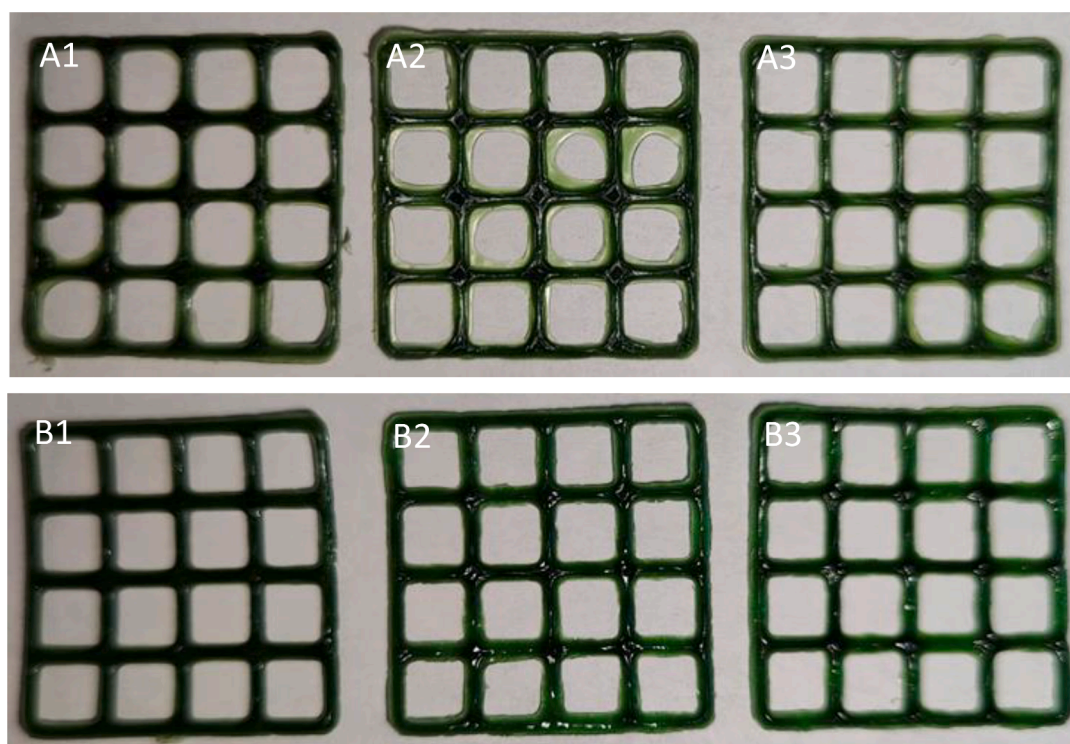


**Fig. 9.** The semi-solid extrusion (SSE) 3D-printed lattices obtained from the aqueous polyethylene oxide (PEO)-eucalypt extract (EE) gels 9 (A1–3) and 10 (B1–3) in three parallel SSE 3D printings.

compared to the reference 12% PEO gel 1 (Table 1 and 2). The viscosity of the aqueous eumulgins containing PEO-EE gels (2–10) were about 2.6–3.7 times lower than the viscosity of a reference 12% PEO gel (Table 2). Therefore, in order to keep the viscosity of the aqueous eumulgins containing PEO-EE gels high enough for SSE 3D printing, the concentration of PEO needs to be increased in the present gels. Therefore, we increased the concentration of PEO in the present gels to 15% and 20% for the subsequent SSE 3D printings of the aqueous PEO-EE gels.

The SSE 3D printing of 15% and 20% PEO gels loaded with EE was significantly improved compared to that obtained with the corresponding aqueous 12% PEO gels loaded with EE. This conclusion was made after the visual inspection of the layout of the corresponding SSE 3D printed lattices and based on the calculations of a  $S_{\text{practical}}/S_{\text{theoretical}}$  ratio (Table 3 and Figs. 3 and 4). The 3D-printed lattices with the low content of EE (0.05 g/10 ml; formulations 2 and 7 in Table 1) were not of good (acceptable) quality. The lattices were very fragile and they were destroyed either by the nozzle of a syringe system, or when they were tried to be removed from the surface of a printing plate. Thus, these formulations (2 and 7) are not applicable for the SSE 3D printing of EE-loaded preparations. All the gels with the EE content of 0.1 g/10 ml (Table 1) were shown to be feasible for SSE 3D printing, but the most suitable aqueous gel formulation for such 3D printing was the gel composing of 20% PEO. The aqueous 20% PEO gel was also found to be a suitable base (platform) for the gels consisting of EE at the concentrations 0.15 g and 0.2 g per 10 ml. The corresponding 3D-printed lattices were uniform in size and shape, and of a good quality (Fig. 4).

The preliminary in-house disintegration test of 3D-printed preparations was performed based on the visual inspection on the disintegration/dissolution of the preparations by placing the samples in purified water ( $22 \pm 2^\circ\text{C}$ ), and verifying that they were completely disintegrated within 10 min (Fig. 10). In the forthcoming studies, the in-vitro disintegration of the preparations will be studied in more detailed by an established disintegration/dissolution method Eur. Ph. (European Pharmacopoeia).

Assay of chlorophylls [30] in the water solutions of the 3D-printed drug preparations showed that total 82–93% of BAS group was released in the present aqueous solution. This suggests a good bioavailability and that the present 3D-printed drug preparations most likely have the antibacterial activity at the level of an original extract (being used for a long time in the treatment of oral infections and wound healing [25]). In SSE 3D printing, we did not use elevated temperatures or other potentially harmful conditions, which could affect the physicochemical stability and/or antimicrobial activity of the extract.

The present aqueous PEO-EE gels (Table 1) were also investigated for the SSE 3D printing of special round-shaped single-unit disc preparations intended for oral administration. All experimental gel formulations (excluding perhaps the gel 5) were feasible for SSE 3D printing. By visual inspection, the 3D-printed PEO-EE disc preparations dissolved rapidly in water within 10–15 min (Fig. 10), thus suggesting the potential applicability as an oral immediate-release delivery system.

It is evident that the present 3D-printed disc preparations with a minor modification can be used as an antibacterial delivery system e.g., for the treatment of oral infections and wound healing. The therapeutic effect of such antibacterial 3D-printed disc preparations could be enhanced by combining EE with the API having a pronounced anti-inflammatory activity in the same final dosage form.

In summary, taking into account the results obtained in the present study, the most promising aqueous PEO-EE gel for a pharmaceutical SSE 3D printing is the formulation 8 consisting EE 10 mg/ml, eumulgins 30 mg/ml and ascorbic acid 20 mg/ml in a 20% PEO gel platform.



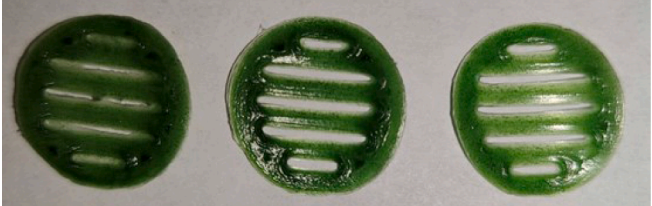




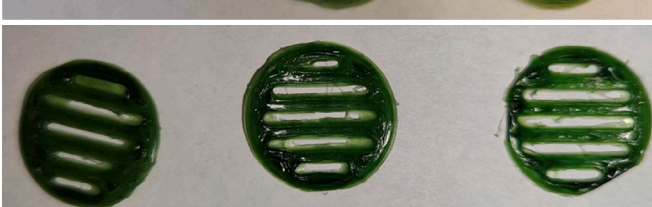
## 5. Conclusions

Novel aqueous PEO gel formulations loaded with antibacterial EE were introduced for pharmaceutical SSE 3D printing applications. The key materials and process parameters of SSE 3D printing affecting the printability of aqueous gels, were identified and verified. The printing quality of the 3D-printed PEO-EE preparations were very good and repeatable, thus showing compatibility of a carrier polymer (PEO) and



**Table 4**


The semi-solid extrusion (SSE) 3D-printed disc preparations obtained from the aqueous polyethylene oxide (PEO)-eucalypt extract (EE) gels in three parallel SSE 3D printings. The compositions of the experimental gels 1–10 are presented in [Table 1](#).

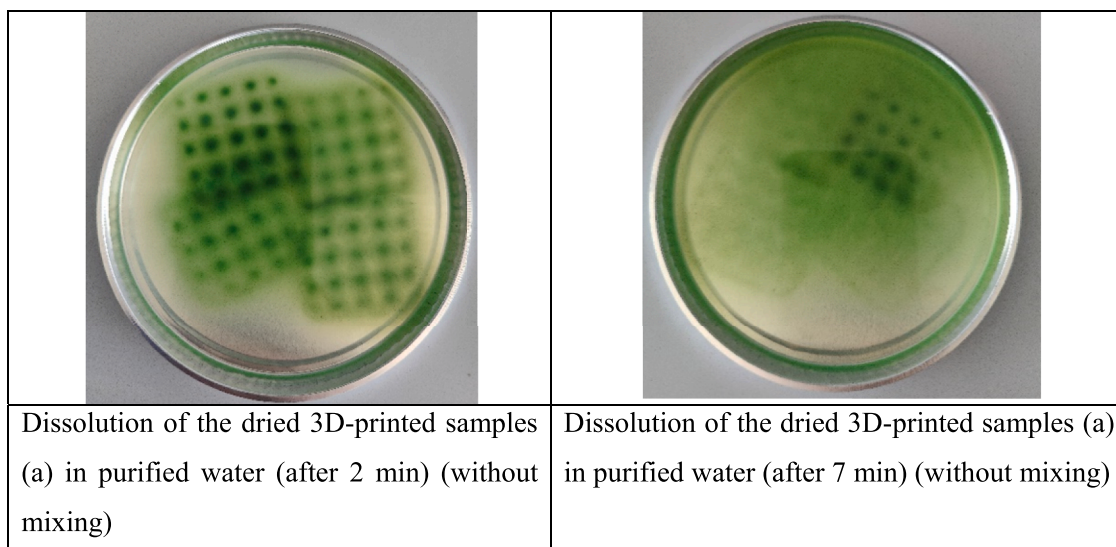
Sample	Weight, g	Photographs
1	0.0450±0.0008	
2	0.0613±0.0107	
3	0.0708±0.0045	
4	0.0750±0.0127	
5	0.0890±0.0005	
7	0.0876±0.0064	
8	0.0959±0.0096	
9	0.0960±0.018	

(continued on next page)



Table 4 (continued)

Sample	Weight, g	Photographs
10	0.0922±0.004	

Fig. 10. Visual inspection of the dissolution of dried 3D-printed preparations in purified water ( $22 \pm 2$  oC).

plant extract (EE). The most feasible aqueous PEO-EE gel for SSE 3D printing is composed of EE 10 mg/ml, eumulgin 30 mg/ml and ascorbic acid 20 mg/ml in a 20% PEO gel platform. The 3D-printed antibacterial PEO-EE disc preparations developed in this study could have potential future medicinal uses in the treatment of infections in oral cavity and in wound healing applications.

#### Declaration of Competing Interest

The authors declare that they have no known competing financial interests or personal relationships that could have appeared to influence the work reported in this paper.

#### Acknowledgements

The Nordic POP (patient-oriented products), a Nordic University Hub project #85352 funded by NordForsk. The authors sincerely thank all the defenders of Ukraine who made the performance of this study possible.

#### Funding

This work was supported by the Estonian Research Council grant (PRG1903), CurifyLabs project (VMVFA22189), and The Estonian Research Council (ETAg) short-term support measure (12.07.2022) for Ukrainian researchers in the Estonian universities' research and development activities; and the European Union in the MSCA4Ukraine project "Design and development of 3D-printed medicines for bioactive materials of Ukrainian and Estonian medicinal plants origin" [ID number 1232466].

#### References

- [1] Viidik L, Seera D, Antikainen O, Kogermann K, Heinämäki J, Laidmäe I. 3D-printability of aqueous poly(ethylene oxide) gels. *Eur Polym J* 2019;120:109206. <https://doi.org/10.1016/j.eurpolymj.2019.08.033>.
- [2] Azad MA, Olawuni D, Kimbell G, Badruddoza AZM, Hossain MS, Sultana T. Polymers for extrusion-based 3D printing of pharmaceuticals: a holistic materials-process perspective. *Pharmaceutics* 2020;12(2):124. <https://doi.org/10.3390/pharmaceutics12020124>.
- [3] Anderspuk H, Viidik L, Olado K, Kogermann K, Jupp Heinämäki J, Laidmäe I. Effects of crosslinking on the physical solid-state and dissolution properties of 3D-printed theophylline tablets. *Ann 3D Print Med* 2021;4:100031. <https://doi.org/10.1016/j.stlm.2021.100031>.
- [4] Mohammed AA, Algahtani MS, Ahmad MZ, Ahmad J. Optimization of semisolid extrusion (pressure-assisted microsyringe)-based 3D printing process for advanced drug delivery application. *Ann 3D Print Med* 2021;2:100008. <https://doi.org/10.1016/j.stlm.2021.100008>.
- [5] Wang Y, Müllertz A, Rantanen J. Structured approach for designing drug-loaded solid products by binder jetting 3D printing. *Eur J Pharm Sci* 2022;178:106280. <https://doi.org/10.1016/j.eurps.2022.106280>.
- [6] Pugliese L, Marconi S, Negrello E, Mauri V, Peri A, Gallo V, Auricchio F, Pietrabissa A. The clinical use of 3D printing in surgery. *Updates Surg* 2018;70:381–8. <https://doi.org/10.1007/s13304-018-0586-5>.
- [7] Yoo JJ, Meng J, Oberpenning F, Atala A. Bladder augmentation using allogenic bladder submucosa seeded with cells. *Urology* 1998;51.
- [8] Luo H, Meyer-Szary J, Wang Z, Sabiniewicz R, Liu Y. Three-dimensional printing in cardiology: current applications and future challenges. *Cardiol J* 2017;24:436–44. <https://doi.org/10.5603/CJ.a2017.0056>.
- [9] Vukicevic M, Mosadegh B, Min JK, Little SH. Cardiac 3D printing and its future directions. *JACC Cardiovasc Imaging* 2017;10. <https://doi.org/10.1016/j.jcmg.2016.12.001>.
- [10] Lin L, Fang Y, Liao Y, Chen G, Gao C, Zhu P. 3D printing and digital processing techniques in dentistry: a review of literature. *Adv Eng Mater* 2019;21:1801013. <https://doi.org/10.1002/adem.201801013>.
- [11] Huri E, Mourad S, Bhide A, Digesu GA. 3D modeling and 3D printing in functional urology: the future perspective. *Int Urogynecol J* 2020;31:1977–8.
- [12] Parikh N, Sharma P. Three-dimensional printing in urology: history, current applications, and future directions. *Urology* 2018;121:3–10. <https://doi.org/10.1016/j.urology.2018.08.004>.
- [13] Lin AY, Yarholiar LM. Plastic surgery innovation with 3D printing for craniomaxillofacial operations. *Mo Med* 2020;117.

- [14] Khaled SA, Burley JC, Alexander MR, Yang J, Roberts CJ. 3D printing of tablets containing multiple drugs with defined release profiles. *Int J Pharm* 2015;494:643–50. <https://doi.org/10.1016/j.ijpharm.2015.07.067>.
- [15] Khaled SA, Burley JC, Alexander MR, Yang J, Roberts CJ. 3D printing of five-in-one dose combination polypill with defined immediate and sustained release profiles. *J Control Release* 2015;217:308–14. <https://doi.org/10.1016/j.jconrel.2015.09.028>.
- [16] Norman J, Madurawe R.D., Moore C.M.V., Khan M.A., Khairuzzaman A. A new chapter in pharmaceutical manufacturing: 3D-printed drug products. 2016.
- [17] Ravanbakhsh H, Bao G, Luo Z, Mongeau LG, Zhang YS. Composite inks for extrusion printing of biological and biomedical constructs. *ACS Biomater Sci Eng* 2021;7(9):4009–26. <https://doi.org/10.1021/acsbomaterials.0c01158>.
- [18] (...) Li S, Jiang Y, Zhou Y, Qin W, Liu Y. Facile fabrication of sandwich-like anthocyanin/chitosan/lemongrass essential oil films via 3D printing for intelligent evaluation of pork freshness. *Food Chem* 2022;370:131082.
- [19] Wang M, Li D, Zang Z, Sun X, Tan H, Si X, Tian J, Teng W, Wang J, Liang Q, Bao Y, Li B, Liu R. 3D food printing: applications of plant-based materials in extrusion-based food printing. *Crit Rev Food Sci Nutr* 2022;62(26):7184–98. <https://doi.org/10.1080/10408398.2021.1911929>.
- [20] Zhou L, Fu J, He Y. A review of 3D printing technologies for soft polymer materials. *Adv Funct Mater* 2020;30:2000187. <https://doi.org/10.1002/adfm.202000187>.
- [21] El Aita I, Rahman J, Breitzkreutz J, Quodbach J. 3D-Printing with precise layer-wise dose adjustments for paediatric use via pressure-assisted microsyringe printing. *Eur J Pharm Biopharm* 2020;157:59–65. <https://doi.org/10.1016/j.ejpb.2020.09.012>.
- [22] Elbadawi M, Nikjoo D, Gustafsson T, Gaisford S, Basit AW. Pressure assisted microsyringe 3D printing of oral films based on pullulan and hydroxypropyl methylcellulose. *Int J Pharm* 2021;595:120197.
- [23] Holland TL, Arnold C, Fowler VG. Clinical Management of *Staphylococcus aureus* Bacteremia: a review. *JAMA* 2014;312(13):1330–41. <https://doi.org/10.1001/jama.2014.9743>.
- [24] Mehraj J, Witte W, Akmatov MK, Layer F, Werner G, Krause G. Epidemiology of *Staphylococcus aureus* nasal carriage patterns in the community. *Curr Top Microbiol Immunol* 2016;398:55–87. [https://doi.org/10.1007/82\\_2016\\_497](https://doi.org/10.1007/82_2016_497).
- [25] Kovalenko VN. Compendium 2020-medicines. Ukraine: MORION: Kiiiv; 2020.
- [26] Koshovi O, Heinämäki J, Raal A, Laidmäe I, Topelius NS, Komissarenko M, Komissarenko A. Pharmaceutical 3D-printing of nanoemulsified eucalypt extracts and their antimicrobial activity. *Eur J Pharm Sci* 2023;106487. <https://doi.org/10.1016/j.ejps.2023.106487>.
- [27] Dhakad AK, Pandey VV, Beg S, Rawat JM, Singh A. Biological, medicinal and toxicological significance of Eucalyptus leaf essential oil: a review. *J Sci Food Agric* 2018;98(3):833–48. <https://doi.org/10.1002/jsfa.8600>.
- [28] Raju G, Maridas M. Composition, antifungal and cytotoxic activities of essential oils of Piper barberi fruits. *Int J Biol Technol* 2011;2:100–5.
- [29] Mieres-Castro D, Ahmar S, Shabbir R, Mora-Poblete F. Antiviral activities of eucalyptus essential oils: their effectiveness as therapeutic targets against human viruses. *Pharmaceuticals* 2021;14(12):1210. <https://doi.org/10.3390/ph14121210>.
- [30] Tumanov VN, Chiruk SL. Qualitative and quantitative methods for studying photosynthesis pigments. GrGU im I Kupala, Grodno 2007.
- [31] Krivoruchko E, Markin A, SamoiloVA. Research in the chemical composition of the bark of *Sorbus aucuparia*. *Ceska Slov Farm* 2018;67(3):113–5.
- [32] Juergen Riegel, Werner Mayer, Yorik van Havre (2001-2021). FreeCAD (Version 0.19.24291). Available from <http://www.freecad.org>.
- [33] Bhawale R, Suryavanshi P, Subham B. Three-dimensional (3D) printing of oral dental films (ODFs) using blended Compactcel® polymers through semi-solid extrusion (SSE) bioprinter. *Bioprinting* 2023;33:e00287. <https://doi.org/10.1016/j.bprint.2023.e00287>.
- [34] European pharmacopoeia. 10th ed. Strasbourg: Council of Europe; 2019.